

Pulsation of the δ Scuti star θ^2 Tau: New multisite photometry and modelling of instability

M. Breger,¹ A. A. Pamyatnykh,^{1,2,3} W. Zima,¹ R. Garrido,⁴ G. Handler,¹ P. Reegen¹

¹*Astronomisches Institut der Universität Wien, Türkenschanzstr. 17, A-1180 Wien, Austria*

²*Copernicus Astronomical Center, Bartycka 18, 00-716 Warsaw, Poland*

³*Institute of Astronomy, Russian Academy of Sciences, Pyatnitskaya Str. 48, 109017 Moscow, Russia*

⁴*Instituto de Astrofísica de Andalucía, CSIC, Apdo. 3004, E-18080 Granada, Spain*

arXiv:astro-ph/0204279v1 17 Apr 2002

Accepted 2002 month day. Received 2002 month day; in original form 2002 month date

ABSTRACT

The results of a multisite photometric campaign of θ^2 Tau are reported. This binary system consists of evolved and main-sequence A stars inside the instability strip. The 12th Delta Scuti Network campaign included 152 hours of high-precision photometry obtained at four observatories. This leads to the derivation of 11 frequencies of pulsation in the 10.8 to 14.6 cd^{-1} range. These frequencies confirm the results from previous Earth-based (1982–1986) as well as satellite (2000) photometry, although amplitude variability on a time scale of several years is present.

We show that at least two high frequencies (26.18 and 26.73 cd^{-1}) are also present in θ^2 Tau. Arguments are given that these high frequencies originate in the main-sequence companion and are not combination frequencies, $f_i + f_j$, from the primary.

Models for both the primary and the secondary components were checked for the instability against radial and nonradial oscillations. All hot models of the primary with $T_{\text{eff}} > 8000\text{ K}$ are stable in the observed frequency range. The best fit between the theoretical and observed frequency ranges is achieved for models with $T_{\text{eff}} \approx 7800\text{ K}$ (or slightly higher), in agreement with photometric calibrations. The instability range spans two or three radial orders in the range p_4 to p_6 for radial modes. Post-main-sequence models (with or without overshooting) are preferable for the primary, but main-sequence models with overshooting cannot be excluded. For the less luminous secondary component the instability range is wider and spans 5 to 7 radial orders from p_2 to p_8 . The observed frequencies lie around radial modes p_5 to p_6 . The main uncertainties of these results are caused by a simple treatment of the convective flux in the hydrogen ionization zone.

Key words: δ Scuti – Stars: oscillations – Stars: individual: θ^2 Tau – Stars: individual: 78 Tau – Techniques: photometric

1 INTRODUCTION

A number of lengthy observing campaigns covering individual δ Scuti variables have shown that the majority of these pulsating variables on and near the main sequence pulsate with a large number of simultaneously excited nonradial p modes. Furthermore, long-term variability of the pulsation amplitudes of these nonradial modes with a time scale of years has been discovered for many, but not all of these nonradial pulsators. The Delta Scuti Network, hereafter called DSN, specializes in multisite observations of these stars. The network is a collaboration of astronomers located at observatories spaced around the globe in order to avoid regular,

daily observing gaps. So far, 21 campaigns have been carried out. The most recent campaign covered BI CMi, for which 29 frequencies of pulsation derived from 1024 hours (177 nights) of photometry were discovered (Breger et al. 2002).

The variability of the star θ^2 Tau was discovered by Horan (1977, 1979) and confirmed by Duerbeck (1978). In order to study the multiple frequencies, the Delta Scuti Network undertook two campaigns (Breger et al. 1987, 1989; the latter is referred to as Paper I). The data could be supplemented by additional measurements by Kovacs & Paparo (1989). Five frequencies of pulsation were detected and interpreted to be due to nonradial pulsation. The size and dis-

tribution of the frequencies suggested p modes with values of $\ell = 0$ to 2. A mode with a higher ℓ value was also detected spectroscopically by Kennelly & Walker (1996). Since the original analysis of the photometric data, new theoretical as well as experimentally determined (Breger et al. 1993) statistical criteria for the acceptance or rejection of additional modes extracted from multisite photometric data have become available. A re-examination of the previous data obtained in the years 1982 to 1986 (Breger 2002, hereafter referred to as Paper II) led to the discovery of ten frequencies in the 1986 DSN data. Nine of these frequencies are also present in the list of twelve frequencies determined during a remarkable study of θ^2 Tau from space (Poretti et al. 2002, hereafter referred to as Paper III): during 2000 August, θ^2 Tau was monitored extensively with the star tracker camera on the Wide-Field Infrared Explorer satellite (WIRE).

θ^2 Tau is a 140.728d binary system with known orbital elements (Ebbighausen 1959, Torres, Stefanik & Latham 1997). The two components have similar temperatures. The primary component is evolved (A7III), while the secondary is fainter by 1.10 mag (Peterson, Stefanik & Latham 1993) and still on the main sequence. Both stars are situated inside the instability strip. It was shown in Paper I that the dominant pulsation modes originate in the primary component because the predicted orbital light-time effects for the primary match the observed shifts in the light curves of up to several minutes. This confirms an expectation from the values of the frequencies ($10 - 15 \text{ cd}^{-1}$), which are incompatible with those of main-sequence δ Scuti stars.

2 NEW GROUND-BASED MEASUREMENTS

In order to eliminate the serious aliasing caused by regular observing gaps, a multisite campaign was organized utilizing the Delta Scuti Network (DSN campaign 12). During 1994 November and December, θ^2 Tau was measured photometrically with the Three-Star-Technique (Breger 1993) at a number of observatories spaced around the globe. Weather conditions, unfortunately, were unfavorable so that data from a number of Asian Observatories were not accurate enough to be included in the present analysis. 152 hours of photometry at four other observatories could be used. These observatories were:

(i) Lowell: The photoelectric photometer attached to the 0.8m reflector at Lowell Observatory, Flagstaff, USA, was used with the Strömgren v and y filters together with a neutral density filter. The observer was W. Zima.

(ii) McDonald Observatory: The 0.9m telescope was used with the y filter. The observer was G. Handler.

(iii) Sierra Nevada Observatory: The 0.9m telescope was used together with v and y filters. The observers were R. Garrido and F. Beichbuchner.

(iv) The 0.6m reflector at the XingLong station of Beijing Astronomical Observatory, China, was used for 9 nights with the V filter. The observers were Li Zhiping, Zhou Aying, and Yang Dawei. More details can be found in Li et al. (1997a), where the Chinese data have already been published, and Li et al. (1997b). We have adopted the Chinese data as published except for the slight editing of a few (obviously) deviant points.

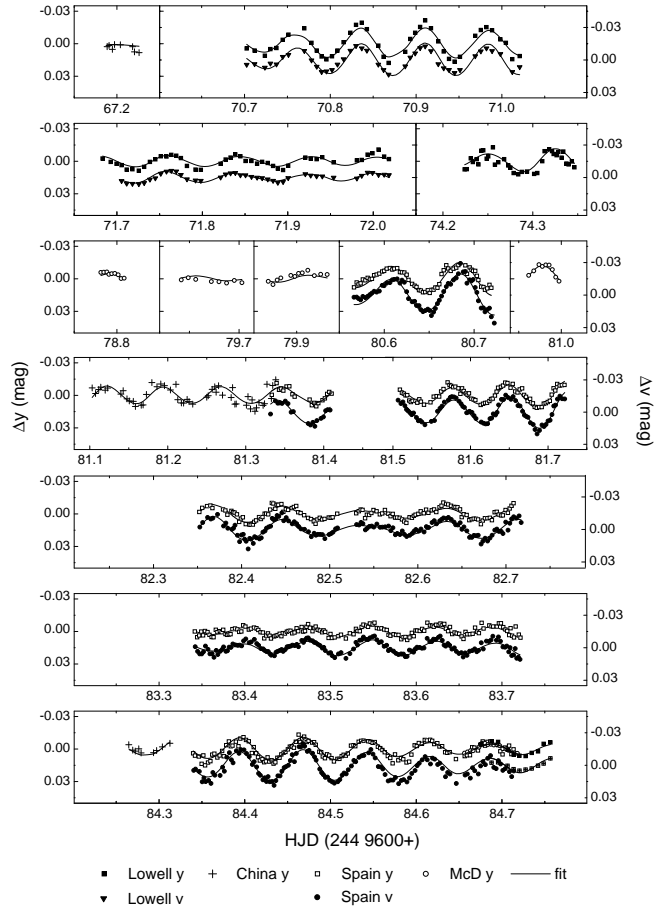


Figure 1. Light curves showing the first half of the 1994 measurements of θ^2 Tau. The curves drawn represent the 13-frequency fit found in a later section.

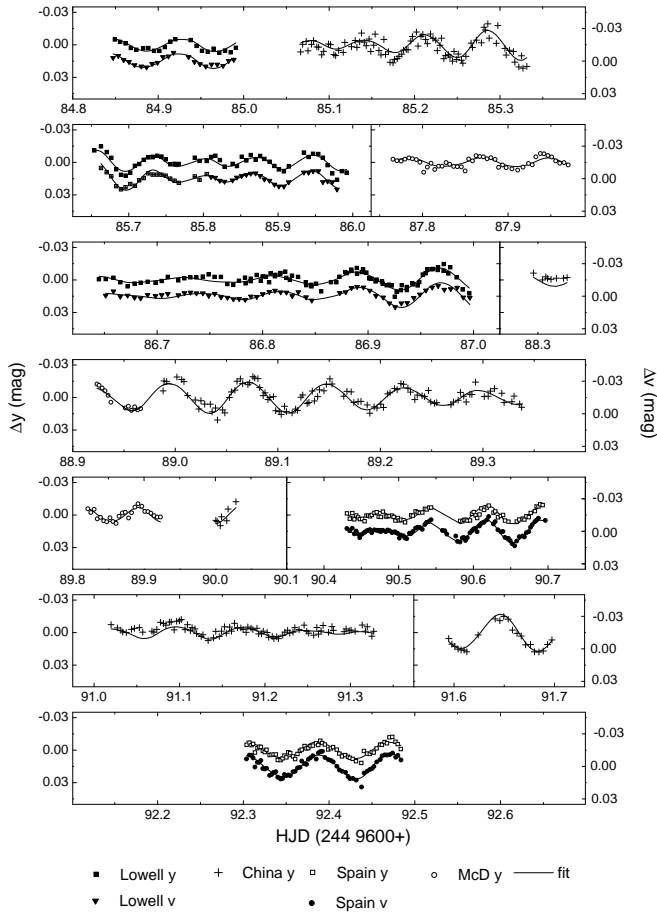
A journal of the photoelectric measurements used is given in Table 1.

All observatories used the same two comparison stars as during the previous DSN campaigns of θ^2 Tau, viz., HR 1422 and HR 1428. No evidence for any variability of these comparison stars was found. We could combine the V and y data, because the y magnitudes are defined to be equal to the V magnitudes. After the standard photometric reductions relative to the two comparison stars, the data from the different observatories needed to be combined. For the initial multifrequency analyses, this was done by subtracting the average relative magnitude of θ^2 Tau at each observatory and then combining the data. Since the multifrequency analyses utilized the fitting of sine curves to the data, the zero-points could then be further adjusted from the values of zero-point of these fits. The times of observation were converted to Heliocentric Julian Date (HJD). We also calculated the light time corrections for the orbital motion of the primary stellar component (see Fig. 6 of Paper I). During this short campaign of 25d, the light time correction is very small and practically constant. Therefore, we have not applied such a correction to the present data. The extinction coefficients were derived separately for each night by using the two comparison stars. For a few short data sets, average extinction coefficients had to be applied.

Table 1. Journal of photoelectric measurements of θ^2 Tau obtained during the 12th Delta Scuti Network campaign

Start HJD	Length hours	Observatory	Start HJD	Length hours	Observatory	Start HJD	Length hours	Observatory
244 9000+			244 9000+					
667.186	0.90	XL	682.347	8.69	SNO	687.761	5.05	McD
670.697	7.77	Lo	683.337	9.25	SNO	688.243	0.85	XL
671.678	8.18	Lo	684.263	1.15	XL	688.919	1.16	McD
674.222	2.93	XL	684.335	9.10	SNO	688.986	8.39	XL
678.776	0.79	McD	684.651	1.61	McD	689.816	2.58	McD
679.637	5.90	McD	684.671	7.70	Lo	689.999	0.68	XL
680.562	3.80	SNO	685.065	6.50	XL	690.426	6.41	SNO
680.957	0.99	McD	685.649	8.24	Lo	691.018	7.38	XL
681.101	5.65	XL	686.640	8.56	Lo	691.590	2.60	McD
681.328	9.45	SNO	686.779	4.75	McD	692.299	4.45	SNO

Lo: Lowell Observatory, USA; McD: McDonald Observatory, USA; SNO: Sierra Nevada Observatory, Spain
 XL: Xing-Long Observatory, China


Figure 2. Light curves showing the second half of the 1994 measurements of θ^2 Tau.

Figures 1 and 2 show the observed light variations of θ^2 Tau together with the 13-frequency fit derived in later sections. The new data will be made available in the Communications in Asteroseismology.

3 METHODS USED TO DETERMINE MULTIPLE FREQUENCIES FROM THE LIGHT CURVES

The pulsation frequency analyses were performed with a package of computer programs with single-frequency and multiple-frequency techniques (PERIOD98, Sperl 1998). These programs utilize Fourier as well as multiple-least-squares algorithms. The latter technique fits a number of simultaneous sinusoidal variations to the observed light variability and does not rely on prewhitening. For the purposes of presentation and initial searches, however, prewhitening is required if the low-amplitude modes are to be seen. Therefore, in the presentation of the results (see below), the various power spectra are presented as a series of panels, each with additional frequencies removed relative to the panel above.

Two observatories also provided measurements in a second filter, viz., the Strömgren v filter. In this filter, the amplitudes of θ^2 Tau are higher by about 30% relative those in the y filter. In power spectra, the location of the peaks in frequency are not affected by mixing data with different amplitudes. Consequently, for the power spectra we have used the data from all filters. The slight phase shift up to 10° in the light curves of δ Scuti stars between the different filters was ignored, since numerical simulations show that for δ Scuti stars the power spectra are not affected by such small shifts.

However, for prewhitening, the data from the two filters had to be treated separately. The multiperiodic fitting of sinusoids to the data relies on the minimization of the residuals between the fit and the observations and requires correct amplitudes. This problem was solved by computing separate solutions for the two colors, which could then be prewhitened.

One of the most important questions in the examination of multiperiodicity concerns the decision as to which of the detected peaks in the power spectrum can be regarded as variability intrinsic to the star. Due to the presence of non-random errors in photometric observations and because of observing gaps, the predictions of standard statistical false-

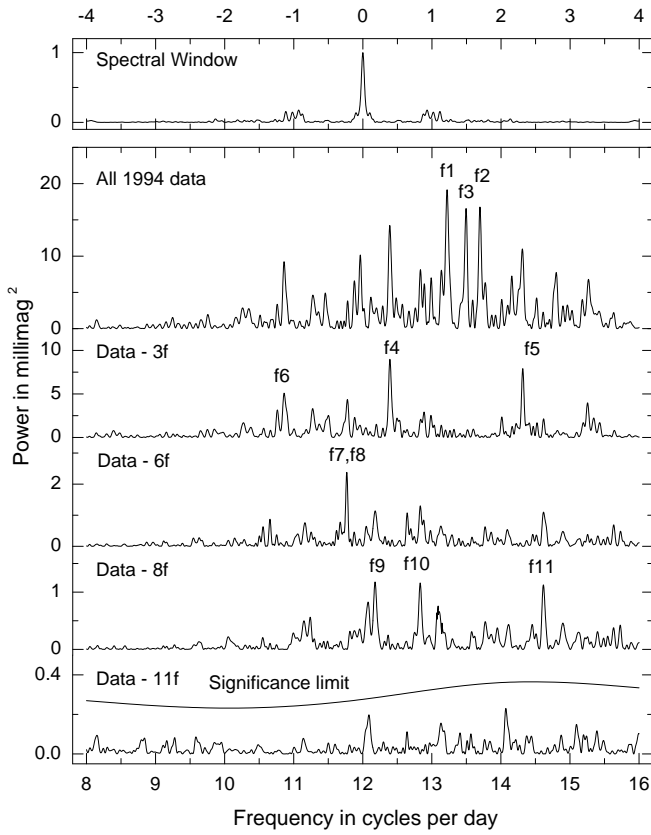


Figure 3. Power spectra of the 1994 photometry of θ^2 Tau. The top panel shows the spectral window, while the other panels present the power spectra before and after prewhitening a given number of frequencies. See text for a discussion of significance levels.

alarm tests give answers which are considered by us to be overly optimistic. In a previous paper (Breger et al. 1993) we have argued that a ratio of amplitude signal/noise = 4.0 provides a useful criterion for judging the reality of a peak. This corresponds to a power signal/noise ratio of 12.6. Subsequent analyses comparing independent data sets have confirmed that this criterion is an excellent predictor of intrinsic vs. possible noise peaks, as long as it is not applied to very small data sets or at low frequencies, where the errors of measurement are far from random. In the present study, the noise was calculated by averaging the amplitudes (oversampled by a factor of 20) over 5 cd^{-1} regions centered around the frequency under consideration.

4 THE MAIN PULSATION FREQUENCIES OF θ^2 TAU DURING 1994

The spectral window of the 1994 data (Fig. 3) is quite clean because the data were collected on three continents, thereby avoiding serious regular day-time observing gaps. Nevertheless, the 1 cd^{-1} aliasing should still be kept in mind, since modes with very small amplitudes might hide in the alias peaks.

The power spectrum of θ^2 Tau was computed from frequency values of zero to the Nyquist frequency. The highest

Table 2. The photometric frequency spectrum of θ^2 Tau during 1994

	Frequency	1994 Amplitudes	
		v filter	y filter
	cd^{-1}	μHz	mmag
			± 0.1
f1	13.230	153.1	4.8
f2	13.694	158.5	5.2
f3	13.484	156.1	3.2
f4	12.397	143.5	3.7
f5	14.316	165.7	3.7
f6	10.865	125.8	2.3
f7	11.770	136.2	2.3:
f8	11.730	135.8	1.2:
f9	12.177	140.9	1.7
f10	12.832	148.5	1.4
f11	14.615	169.2	1.9
			1.2

power levels were found in the 10 to 16 cd^{-1} region. An additional band of power was found in the 26 to 30 cd^{-1} region and will be examined in a later section. The power spectra in the 8 to 16 cd^{-1} region are presented in Fig. 3. The second panel from the top shows the dominant three frequencies, which have been found in all other photometric campaigns as well. The next panel shows the power spectrum after prewhitening of the main three frequencies. Three additional peaks are detected without any problems.

The power spectrum of the data after prewhitening six frequencies (Data - 6f) presents a small problem: the dominant peak may be double. The peak at 11.770 cd^{-1} , called f_7 , is strong and its frequency easily determined. Removal of this mode leaves another peak at 11.730 cd^{-1} at a lower amplitude. The frequency separation of 0.04 cd^{-1} is at the limit of frequency resolution of the present data set. This prevents us from applying the powerful phasing-amplitude test to distinguish between two independent close frequencies and the artifacts caused by a single frequency with variable amplitudes (see Breger & Bischof 2002). Fortunately, it is not necessary here to prove the existence of a frequency doublet: both frequencies have been seen before in the WIRE data (Paper III), while the weaker component in the 1994 data was already detected in the 1986 data (Paper II). We therefore accept the reality of the two close frequencies, f_7 and f_8 .

Three additional frequencies are found in the 1994 data. Further peaks are below the statistical threshold (bottom panel of Fig. 3).

The adopted frequencies and amplitudes are shown in Table 2. The uncertainties in amplitude were calculated from the standard formulae given in Breger et al. (1999), based on the assumption of random observational errors and no aliasing. The uncertainties of the amplitudes of f_7 and f_8 are larger because these two modes are very close in frequency. Because the separation of two frequencies is at the resolution limit of the present data set, the computed size of the amplitude of one mode is somewhat affected by the presence of the other mode (the so-called pumping effect). These amplitudes are therefore marked with a colon.

The new solution fits the observed data well, as shown

in Figs. 1 and 2. The good fit is also demonstrated by the value of the average residual per single measurement of ± 2.7 mmag in v and ± 3.2 mmag in y .

5 COMPARISON WITH PREVIOUS STUDIES

There now exist three large photometric studies of θ^2 Tau: the present study based on 1994 multisite data, the reanalysis of the 1982–1986 multisite campaigns (with emphasis on the 1986 data, Paper II), and the WIRE satellite study from space (Paper III). Each photometric study detected between 10 and 12 frequencies. The excellent agreement between the frequencies found in these independent studies is remarkable.

5.1 The main modes: f_1 to f_5 , f_8 to f_{11}

These 9 frequencies were detected in all three studies, but with variable amplitudes. While during the years 1982, 1983 and 1986, the mode at 13.23 cd^{-1} is dominant in each of these years, during 2002 the 13.69 cd^{-1} frequency became dominant.

5.2 The mode at 10.86 cd^{-1} : f_6

The mode at 10.86 cd^{-1} is present with amplitudes in excess of 1.0 mmag in both the 1994 and 2000 data, but appears to be absent (y amplitude ≤ 0.3 mmag) during 1986.

5.3 The $11.73/11.77 \text{ cd}^{-1}$ doublet: f_7 and f_8

The frequency separation of this close frequency pair is near the frequency resolution given by the 25d length of the 1994 data set as well as that of the 1986 and the WIRE results. In the WIRE data, the two frequencies are both present with similar amplitudes. During 1994, 11.77 cd^{-1} is dominant but the other peak is also visible. In the 1986 data, we can only see the other, lower-frequency mode. The 1982/3 data offer higher frequency resolution, but are not useful for the study of the pair because of a higher noise level.

We conclude that both modes are probably present. The strong amplitude variability of these modes may be intrinsic to the star or an artefact caused by poor frequency resolution.

5.4 Additional frequencies at 12.70 and 13.81 cd^{-1}

Two additional frequencies are seen at statistically significant levels in only one of the three data sets:

(i) The 1986 data reveal an additional mode at 13.81 cd^{-1} , which has not been seen before. The power spectrum of the WIRE residuals shows a peak at 13.83 cd^{-1} (see Fig. 6 of Paper III) and is therefore probably also present in that data set.

(ii) A mode at 12.70 cd^{-1} was also found by WIRE, which is not affected by 1 cd^{-1} aliasing and is therefore not affected by another mode near 11.73 cd^{-1} . A formal solution with the 1994 data including this frequency yields a minuscule amplitude of 0.3 mmag. The mode may be present in the 1986 data, because in the power spectrum a small peak at

an amplitude level of ~ 0.5 mmag is seen at that frequency value, but below the level of significance. Numerical simulations suggest that the slight 1 cd^{-1} aliasing still present in the multisite ground-based campaign data is not responsible for the computed small (or zero) amplitudes in 1986 and 1994.

5.5 Amplitude ratios and phase differences

The variability measurements from Lowell and Sierra Nevada Observatories were obtained with the two v and y filters of the $uvby\beta$ system in order to compare amplitude ratios and phase differences in different colors. Especially the phase differences for different pulsation modes allow a discrimination between different ℓ values, but extensive measurements of extremely high photometric accuracy are required. The present study, regrettably, is not large enough for reliable mode identifications. In fact, the formal uncertainties in the phase differences are less than $\pm 3.0^\circ$ for only three modes: f_1 , f_2 and f_4 . All three modes give similar amplitude ratios with an average value of $A_v/A_y = 1.25 \pm 0.05$. For these modes the phase differences, $\phi_v - \phi_y$, are -7° with uncertainties of $\pm 2^\circ$ for the first two modes and $\pm 3^\circ$ for f_4 .

6 THE HIGH-FREQUENCY REGION

An additional frequency region with power in excess of the expected noise occurs in the 26 to 30 cd^{-1} region. This is shown for the 1994 data in the top panel of Fig. 4. Several promising peaks exist, but do not reach the amplitudes required for a statistically certain discovery of a new pulsation frequency, viz., amplitude signal/noise ratios ≥ 4.0 .

The statistics can be improved considerably by examining other photometric data in the literature, viz. the data obtained during 1982, 1983 and 1986 (see Paper I). For the 1982/1983 and 1986 photometry, we have prewhitened the variability in the low-frequency domain and computed power spectra in the high-frequency region. This is also shown in Fig. 4. The peak at 26.2 cd^{-1} is present in all data sets. In spite of the small amplitude of 0.6 mmag, the detections are statistically significant in two of the three data sets. An additional peak at 26.7 cd^{-1} is also statistically significant in the 1982–1986 data, but not seen in 1994. On the other hand, the most promising peak in 1994, 28.9 cd^{-1} , is not seen in the earlier data. Since its detection is not statistically significant in any (including a combined 1982–1994) data set, it is not adopted by us.

It is interesting that the 26.2 cd^{-1} variability was also seen independently by the WIRE satellite: Poretti et al. in Paper III ascribe this to a spurious term caused by the duty cycle and experimental errors. In view of the present detection of the same frequency in earth-based data, we can rule out an experimental origin and conclude that these high frequencies originate in θ^2 Tau.

Table 3 lists the amplitudes for the two significant modes.

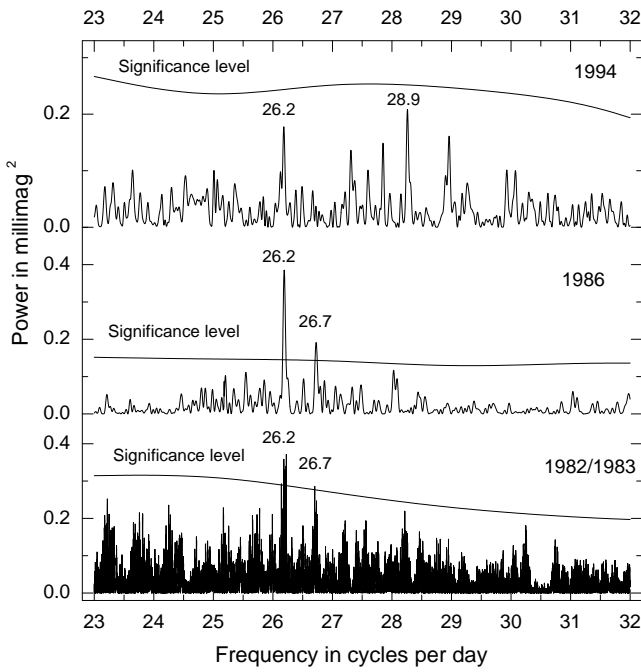


Figure 4. Power spectra in the high-frequency region. The frequency at 26.2 cd^{-1} is present in all data sets, while 26.7 cd^{-1} is present in both the 1986 and 1982/3 data sets.

Table 3. Variability of θ^2 Tau at high frequencies

	Frequency		Amplitudes ¹			
	cd^{-1}	μHz	1982/83	1986	1994 <i>v</i>	1994 <i>y</i>
f_{12}	26.184	303.1	±0.1	±0.1	±0.1	±0.1
f_{13}	26.732	309.4	0.6	0.6	0.5	0.4
			0.5	0.5	0.1	0.1

¹ Note that an amplitude of 0.1 mmag does not represent a statistically significant detection.

6.1 Could the high frequencies be combination or harmonic frequencies?

δ Scuti stars often show combination frequencies, $f_i \pm f_j$, as well as slightly nonsinusoidal light curves leading to $2f_i$ peaks in the power spectrum. These peaks are, of course, situated at high frequencies and are characterized by amplitudes smaller than a factor of ten (or more) relative to those of f_i . Since θ^2 Tau has its main variability in the $11-15 \text{ cd}^{-1}$ range, combination frequencies/ $2f$ terms would be found in the $22-30 \text{ cd}^{-1}$ region and therefore provide a potential explanation.

The frequencies of the potential high-frequency candidates can be easily calculated from $f_i \pm f_j$ and $2f_i$. Such have been detected even in low-amplitude δ Scuti stars such as 4 CVn (Breger et al. 1999) and XX Pyx (Handler et al. 1996, 2000).

The value of the main high frequency, f_{12} at 26.184 cd^{-1} , cannot be identified with the frequency of a combination of any two modes listed in Table 1. We conclude that it is not a combination frequency. On the other hand, f_{13} at 26.732 cd^{-1} , is in the vicinity of two potential combi-

nations, $f_1 + f_3 = 26.714$ and $f_4 + f_5 = 26.713 \text{ cd}^{-1}$. Although the 1982–1986 data have an excellent frequency resolution due to the 1000+ day span, the data contain long gaps, leading to the possibility of spectral leakage. We can see smaller peaks near 26.714 cd^{-1} , so that some of the power at 26.732 cd^{-1} may be spectral leakage from combination frequencies. The important question concerns the physical origin of the combination terms, e.g., are these combination frequencies just combination terms or are new modes excited by resonance at frequencies near those of the combination frequencies? Garrido & Rodriguez (1996), in their study of combination frequencies, point out that the phasing of these combination terms might allow us to distinguish between the two possibilities. However, for low-amplitude δ Scuti stars, accurate phasing of combination terms are observationally difficult to determine and the question cannot be examined further at this stage.

Observations of δ Scuti stars (and other pulsating variables) with known combination frequencies show that the amplitudes of the combination terms are a function of the amplitudes of the two frequencies involved in the combination terms. We can estimate the size of the combination terms, $f_i + f_j$ and $2f_i$ from the Garrido & Rodriguez analysis as well as the observations of XX Pyx, 4 CVn and BI CMi (Breger et al. 2002) and calculate expected amplitudes small than 0.1 mmag. This is an order of magnitude smaller than observed. The amplitude argument, therefore, does not support an identification of the two frequencies as combination modes.

We conclude that the main peak, f_{12} cannot be identified as a combination frequency, while such an explanation is unlikely for f_{13} .

6.2 Pulsation in a δ Scuti binary companion

θ^2 Tau is a 140.728d binary system with two components of similar temperature. Peterson, Stefanik & Latham (1993) have shown that the secondary is fainter by 1.10 mag and still on the main sequence. Both stars are situated inside the instability strip. It was shown in Paper I that the dominant pulsation modes originate in the evolved primary component because the predicted orbital light-time effects for the primary match the observed shifts in the light curves of up to several minutes. This confirms an expectation from the values of the frequencies ($10-15 \text{ cd}^{-1}$) which are incompatible with those of main-sequence δ Scuti stars.

What would be the expected frequencies of pulsation of the main-sequence secondary? Although δ Scuti stars pulsate with many simultaneously excited modes of pulsation, the average time-scale obeys a period–luminosity relation of the form, $M_v \sim -3.05 \log P$ (see Breger 2000). We can now apply the known magnitude difference between the components to provide a rough estimate of the frequencies expected for the secondary. The magnitude difference of 1.10 mag shifts the $11-15 \text{ cd}^{-1}$ range of the primary to $25-33 \text{ cd}^{-1}$, which agrees with the band of power seen in the power spectrum.

The light of the secondary is heavily diluted by the light from the primary, which is 1.1 mag brighter than the secondary. Consequently, the amplitudes of pulsation of the secondary are reduced to one fourth of their intrinsic values. If our interpretation is correct, then the secondary would have

V amplitudes of about 0.5 mmag in combined light, or 2 mmag in the star alone. The hypothesis that these modes come from the secondary can be tested: the orbital motions produce light-time shifts of several minutes. Regrettably, the observed amplitudes are too small to obtain the required accuracy in the phasing at different orbital times.

7 PULSATION MODELS FOR θ^2 TAU

In order to examine the nature of the pulsations of θ^2 Tau in more detail, the physical parameters for the two stars forming the binary system need to be determined. A recent summary of different determinations of global parameters of θ^2 Tau can be found in de Bruijne et al. (2001). Torres et al. (1997) used the orbital parallax to derive absolute visual magnitudes, M_v , of 0.37 and 1.47 for the two components. Similar values, 0.48 and 1.58, are obtained by de Bruijne et al. (2001) and Lebreton et al. (2001) from Hipparcos dynamical parallax. Both stars have similar temperatures and its value can be obtained from the Moon & Dworetsky (1985) calibration of $uvby\beta$ photometry, viz., $T_{\text{eff}} = 7950$ K. This value is lower than the value of 8200 K adopted by Breger et al. (1987) as well as others, since the older model-atmosphere calibrations of $uvby\beta$ tended to overestimate the temperatures of A stars. Using a calibration of the UBV photometry, de Bruijne et al. (2001) derive $T_{\text{eff}} = 7980$ K for the primary and $T_{\text{eff}} = 8230$ K for the secondary component.

The Moon & Dworetsky (1985) calibration also allows us to derive a $\log g = 3.69$ from the $uvby\beta$ photometry of the combined light of the two stars. Correction of the measured Balmer discontinuity, c_1 , for the less evolved secondary places our estimate for the primary near $\log g = 3.55$.

This implies a considerably higher evolutionary status than that deduced by Torres et al., who adopted $\log g = 4.0$. However, our value is consistent with the position of the star in the Hertzsprung–Russell Diagram for the Hyades cluster as well as the known luminosity (see above). We can also derive the $\log g$ value from the known mass, luminosity and temperature: for a mass of 2.42 solar masses for the primary (Torres et al.) a $\log g$ value of 3.63 is derived, in agreement with the value found above from $uvby\beta$ photometry.

Finally, this as well as similar studies neglect the effect of rotation and aspect, which affect the choice of the appropriate values for temperature, luminosity and gravity (e.g., see Pérez Hernández et al. 1999).

7.1 Method of computation

The method of computation of stellar evolution and pulsation was the same as in our other studies of δ Scuti stars (see Pamyatnykh 2000 and references therein). In particular, we used the latest version of the OPAL opacities (Iglesias & Rogers 1996) supplemented with the low-temperature data of Alexander & Ferguson (1994). Also, we used an updated version of the OPAL equation of state (Rogers et al. 1996), viz., version EOS2001, which was copied from the OPAL data library*.

The computations were performed starting with chemically uniform models on the ZAMS, assuming an initial hydrogen abundance $X = 0.716$, a helium abundance $Y = 0.26$ and a heavy element abundance $Z = 0.024$. These values correspond to recent estimates of the chemical composition of the Hyades (Perryman et al. 1998, Lebreton et al. 2001). We also tested models of somewhat different chemical composition, with slightly higher metallicity or with higher helium content ($X = 0.723$, $Y = 0.25$, $Z = 0.027$; $X = 0.686$, $Y = 0.29$, $Z = 0.024$).

We computed models with and without overshooting from the convective core. In the first case, the overshooting distance, d_{over} , was chosen to be $0.2 H_p$, where H_p is the local pressure scale height at the edge of the convective core. Examples of evolutionary tracks for δ Scuti models computed with and without overshooting are given by Breger & Pamyatnykh (1998) and Pamyatnykh (2000). In the stellar envelope the standard mixing-length theory of convection with the mixing-length parameter $\alpha = 1.6$ was used. This value was also used by Perryman et al. (1998) and Lebreton et al. (2001), who derived α from the calibration of the solar-model radius.

Uniform (solid-body) stellar rotation and conservation of global angular momentum during evolution from the ZAMS were assumed for all computations. These assumptions were chosen due to their simplicity. The influence of rotation on the evolutionary tracks of δ Scuti models was demonstrated by Breger & Pamyatnykh (1998) and Pamyatnykh (2000). In most cases the initial equatorial rotational velocity on the ZAMS was chosen to be 100 km/s.

The linear nonadiabatic analysis of low-degree oscillations ($\ell \leq 2$) was performed using the code developed by Dziembowski (1977). The effects of slow rotation on oscillation frequencies were treated up to third order in the rotational velocity (Dziembowski & Goode 1992, Soufi et al. 1998).

The main aim of the present theoretical study was to check the instability of models of both stellar components of θ^2 Tau for the whole range of allowed values of mass or gravity, effective temperature and luminosity and to outline possible asteroseismological constraints to the models. We did not attempt to construct any model which fits quantitatively the observed and the theoretical frequency spectra of excited multiperiodic oscillations.

As a first step, we tried to fit the observed and theoretical frequency ranges of the unstable modes. The main uncertainty of such a study is the unsatisfactory description of convection in the stellar envelope and its interaction with pulsations. The fact that convection may influence the instability of stars not only near the Red Edge but almost in the whole classical instability strip was discussed by Stellingwerf (1984) in connection with the problem of the determination of helium abundance in globular clusters from the temperature at the Blue Edge of the RR Lyrae instability domain. δ Scuti stars are generally hotter than RR Lyrae stars, but even in this part of the instability strip convection influences the onset of the instability for low overtones of radial and nonradial oscillations. Fig. 9 of Pamyatnykh (2000) demonstrates that convection significantly displaces the radial fundamental Blue Edge to hotter temperatures due to increased driving in the hydrogen ionization zone which is more extended than in the radiative models. A part of this contribu-

* <http://www-phys.llnl.gov/Research/OPAL/opal.html>
<ftp://www-phys.llnl.gov/pub/opal/eos2001/>

tion to the driving may also be caused by the generally-used assumption that the convective flux does not vary during an oscillation cycle. This simple assumption is probably incorrect in the hydrogen convection zone. Therefore, the reality of the additional convective destabilization in the outer hydrogen zone must be examined by using a nonlocal time-dependent treatment of convection. First promising results in this direction (see Michel et al. 1999, Houdek 2000) exist. Note that the total driving in a δ Scuti star (with main contribution due to the κ mechanism operating in the second helium ionization zone) only slightly exceeds the total damping. Therefore even small contributions to the driving are important.

Due to these uncertainties we consider our results as preliminary and our models as test models. Nevertheless, even with such a simple description of the convection we may have a possibility to constrain the stellar parameters from instability studies.

7.2 Results for test models

In Fig. 5 we show evolutionary tracks for selected models, computed by taking overshooting from the stellar convective core into account. The models with effective temperature $T_{\text{eff}} = 8000, 7900$ and 7800 K, in which we study the oscillations, are marked by filled circles. The luminosities of the higher and the lower-mass models approximately correspond to the luminosity of the primary and secondary stellar components, respectively.

For the primary component, we have chosen models at the beginning of the post-main-sequence (hereafter called post-MS) expansion stage, which burn hydrogen in a thick shell just after full hydrogen exhaustion in the stellar core. This evolutionary stage of the primary was proposed earlier by Królikowska (1992) for a significantly hotter model of about 8200 K without overshooting. Moreover, we studied slightly more massive models of similar effective temperature and luminosity in the MS stage as well as post-MS models without overshooting.

The secondary component, which is fainter by approximately 1.1 mag (which corresponds to the difference by 0.44 in $\log L$ between the components) is a main-sequence star with hydrogen burning in the convective core.

In Fig. 5 we also plot the Blue Edges of the instability strip taken from Pamyatnykh (2000), which were computed for nonrotating models without overshooting for $X = 0.70$, $Y = 0.28$, $Z = 0.02$ and with an assumed mixing-length parameter $\alpha = 1.0$. The general Blue Edge is defined as the hotter envelope of unstable overtones, from radial mode p_8 (seventh overtone) near the ZAMS to mode p_5 (fourth overtone) for highest luminosities or smallest gravities in the figure (see Fig. 3 in Pamyatnykh 2000). The Blue Edge for the radial fundamental mode lies approximately in the center of the δ Scuti instability strip.

An additional study of the instability along the $2.5 M_{\odot}$ evolutionary track shows that the best theoretical general Blue Edge for $X = 0.716$, $Y = 0.26$, $Z = 0.024$ will be located very close to the blue edge shown in Fig. 5, because the differences in the rotational velocity and in the overshooting efficiency do not influence the position of the Blue Edges and because the differences in the helium abundance are small. Moreover, convection has only a minor influence

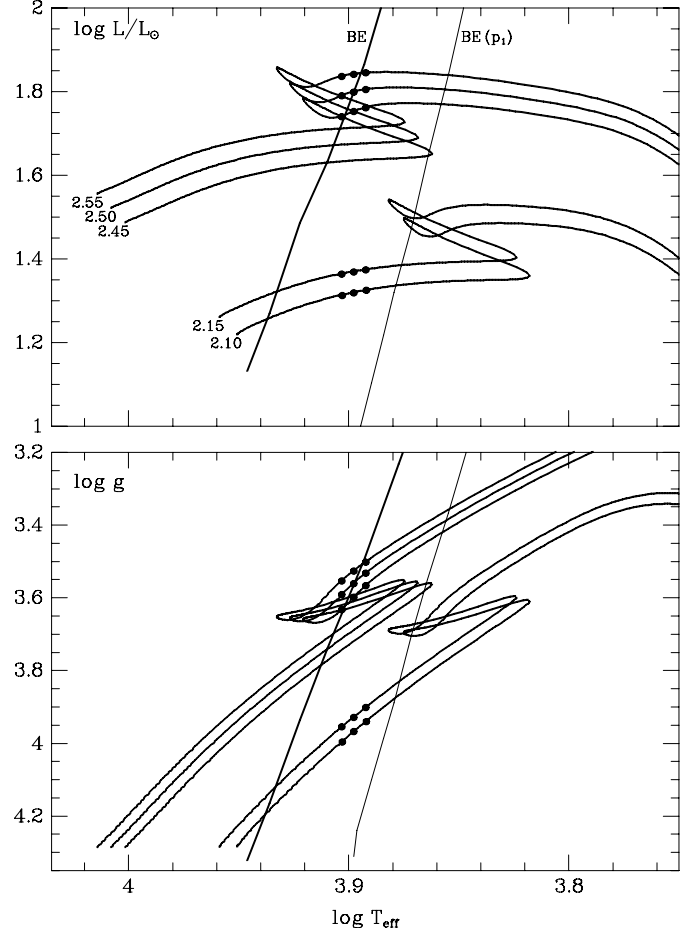


Figure 5. Evolutionary tracks for indicated values of M/M_{\odot} . Test models with effective temperature $T_{\text{eff}} = 8000, 7900$ and 7800 K for the primary and the secondary component of θ^2 Tau are marked by filled circles. All models were computed for an initial hydrogen abundance $X = 0.716$, a helium abundance $Y = 0.26$ and a heavy element abundance $Z = 0.024$. A mixing-length parameter of convection $\alpha = 1.6$ was used. Overshooting from the stellar convective core was taken into account with an overshooting distance $d_{\text{over}} = 0.2 H_p$. The equatorial rotational velocity on the ZAMS was chosen to be 100 km/s. The almost vertical lines show the general Blue Edge of the instability strip and the Blue Edge of the radial fundamental mode, p_1 , as computed for a standard chemical composition (Pamyatnykh 2000).

on the position of this hot general Blue Edge (see Fig. 9 in Pamyatnykh 2000). For the fundamental radial mode the best Blue Edge will be hotter by $0.008 - 0.009$ in $\log T_{\text{eff}}$. This is mainly due to a higher value of the mixing-length parameter.

From Fig. 5 we immediately obtain a strong constraint on the possible effective temperature of the primary of θ^2 Tau. All models with $\log(L/L_{\odot}) > 1.67$ and $\log T_{\text{eff}} > 3.907$ ($T_{\text{eff}} > 8070$ K) are stable in all modes. A MS model of $2.5 M_{\odot}$ on the Blue Edge ($T_{\text{eff}} = 8070$ K) is marginally unstable in radial mode p_6 with the frequency 18.74 cd^{-1} , which is well outside the observed frequency range. We can conclude that only significantly cooler models can pulsate with the observed frequencies in the 10.8 to 14.6 cd^{-1} range.

This conclusion is confirmed by computation of oscillations of the selected test models for the primary of θ^2 Tau.

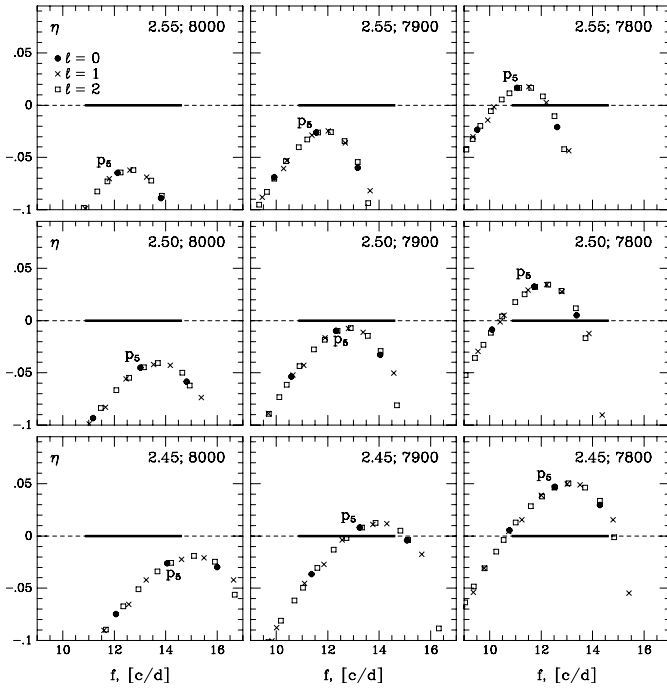


Figure 6. Normalized growth rates, η , plotted against frequency, f , in test models of the primary component of θ^2 Tau. Positive values of η correspond to unstable modes. The values of M (in solar units) and T_{eff} are given in each panel. The position of the models in the HR diagram is shown in Fig. 5. Models were calculated with initial abundances $X = 0.716$, $Y = 0.26$, $Z = 0.024$ and $V_{\text{rot}}(\text{ZAMS}) = 100$ km/s. The symbol p_5 is plotted near the corresponding radial overtone. The thick horizontal line shows the range of frequencies (10.865 to 14.615 cd^{-1}) observed for the primary component of θ^2 Tau.

In Fig. 6, the normalized growth rates of radial and nonradial modes are plotted against frequency for all nine higher-mass models which are marked in Fig. 5. Only axisymmetric modes ($m = 0$) are shown. The independence of the growth rate on the spherical harmonic degree, ℓ , is a typical feature of modes excited by the κ mechanism. The rotational velocities of the models are 81 to 86 km/s. The rotational splitting of the modes can extend the frequency range by approximately 0.5 c/d on both sides. We can see that excited frequencies of the $2.45 M_{\odot}$ model with $T_{\text{eff}} = 7800$ K are in excellent agreement with the observed frequency range. The frequency range of unstable modes spans three radial orders from p_4 to p_6 for radial modes (mode p_4 is marginally unstable).

As was noted already, the results are sensitive to the treatment of convection. For example, if we use a mixing-length parameter $\alpha = 2.0$ instead of $\alpha = 1.6$, the frequency range of unstable modes for $2.45 M_{\odot}$ model with $T_{\text{eff}} = 7800$ K is extended by 1 c/d on both sides. Moreover, our assumption about the unperturbed convective flux during an oscillation cycle is not fulfilled inside the hydrogen convective zone and may result in artificial additional driving in this zone. Therefore, these preliminary results must be considered with caution.

Similar results were obtained for the models without overshooting, the best fitting is achieved in this case for $2.50 M_{\odot}$ model with $T_{\text{eff}} = 7800$ K. Also, for slightly more

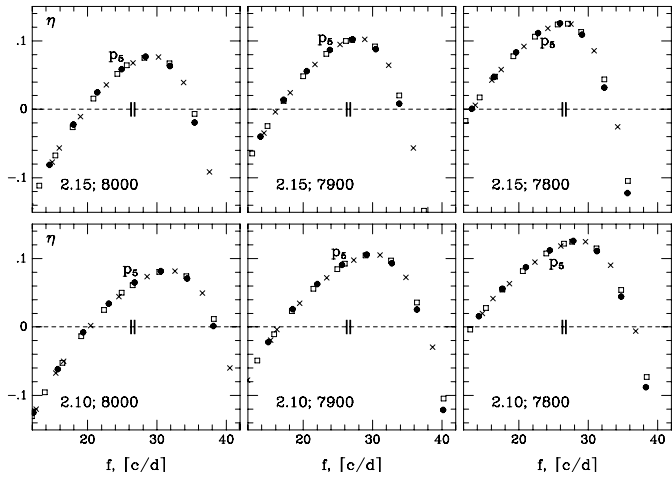


Figure 7. The same as in Fig. 6 but for test models of the secondary component. Short vertical lines mark the observed frequencies 26.184 and 26.732 cd^{-1} .

massive MS models with overshooting, we obtained a good agreement between the observed and the theoretical frequency ranges. The parameters of some models are given in Table 4 below.

In Fig. 7 we show the normalized growth rates in test models of the secondary component. These models are also marked in Fig. 5. As for the primary, we used models with effective temperatures from 7800 to 8000 K. The frequency range of unstable modes is much wider for these less luminous models: it spans 5 to 7 radial orders from p_2 to p_8 . The observed frequencies lie near or between radial modes p_5 to p_6 , which are unstable in the whole range in effective temperature.

In Table 4 we summarize parameters of the best test models. We can see that both MS and post-MS models for the primary with $T_{\text{eff}} = 7800$ K can fit the observed frequency range. The values of the surface gravity and luminosity of all three models are similar. In the computation of the evolution of the MS model P1, the initial equatorial rotational velocity on the ZAMS was chosen to be 80 km/s. (Rotation does not affect our theoretical results significantly, but it may influence the photometric calibrations.) The total number of unstable modes of $\ell \leq 2$ is equal to 37 in the MS model P1, 77 and 56 in the post-MS models P2 and P3, respectively.

Note that the post-MS evolution of models for the primary is much faster than the MS evolution of the less massive secondary. For example, in Fig. 5 all models of $2.45 M_{\odot}$ with $T_{\text{eff}} = 8000$ K, 7900 K and 7800 K (the last model is just model P3) have the same age 695 Myr. These models correspond to stars which are slightly older than the Hyades (650 Myr, Lebreton et al. 2001). On the other hand, the models without overshooting may correspond to stars younger than the Hyades: the age of $2.50 M_{\odot}$ models is 595 Myr. The best model for the primary may therefore be one with slightly weaker overshooting than that of model P3.

The inferred age of the secondary star can be adjusted to the age of the primary as well as to that of the Hyades cluster. This is possible because of the slower main-sequence evolution of the secondary and due to the fact that corresponding models of different effective temperatures fit the

Table 4. Parameters of the best test models of θ^2 Tau which fit the observed frequency ranges. Models of 2.65 , 2.50 and $2.45 M_\odot$ correspond to the primary component, models of $2.10 M_\odot$ correspond to the secondary component. The symbols have their usual meanings (see text). The last column gives the frequency range, in cycles per day, of unstable modes for each model.

Model	M/M_\odot	Ev. Stage	Age [Myr]	T_{eff}	$\log L$	$\log g$	V_{rot}	d_{overt}	Frequency range
P1	2.65	MS	535	7800	1.792	3.58	60	0.2	10.7 – 15.4
P2	2.50	post-MS	595	7800	1.780	3.56	83	0.0	10.5 – 14.6
P3	2.45	post-MS	695	7800	1.762	3.57	84	0.2	10.6 – 14.9
S1	2.10	MS	667	7900	1.319	3.97	91	0.2	13.0 – 37
S2	2.10	MS	704	7800	1.325	3.94	90	0.2	16.5 – 38

observed frequencies quite well. As an example, models of $2.10 M_\odot$ with $T_{\text{eff}} = 8000$ K, 7900 K and 7800 K have the ages 625, 667 and 704 Myr.

Moreover, we tested some models of different chemical composition. If we choose the estimated values for the helium content (Lebreton et al. 2001) and metallicity (Lastennet et al. 1999), the chemical compositions become $X = 0.723$, $Y = 0.25$, and $Z = 0.027$. The results for these models are very similar to those computed above for $X = 0.716$, $Y = 0.26$, $Z = 0.024$.

Models with $X = 0.686$, $Y = 0.29$, $Z = 0.024$ are somewhat more luminous for a given mass, e. g., the track of $2.45 M_\odot$ almost coincides with the track of $2.55 M_\odot$ computed with $X = 0.716$, $Y = 0.26$, $Z = 0.024$. The models are also pulsationally more unstable and the range of unstable modes is somewhat wider due to higher helium abundance. As a consequence, the MS model of $2.45 M_\odot$ with $T_{\text{eff}} = 7900$ K can be unstable in the observed frequency range and also at slightly higher frequencies. The luminosity of this model, $\log(L/L_\odot) = 1.71$, agrees with the estimates from the orbital and dynamical parallaxes.

8 CONCLUSION

The DSN campaign 12, carried out during 1994 at four observatories, resulted in 152 hours of high-precision photometry. 13 frequencies of pulsation were derived from the data. These frequencies confirm the results from previous Earth-based (1982–1986) as well as satellite (2000) photometry, although amplitude variability on a time scale of several years is present.

While the detected modes in the 10 – 15 cd $^{-1}$ range probably all originate in the primary, the higher frequencies with small amplitudes probably originate in the δ Scuti-type of variability of the main-sequence companion.

We constructed evolutionary models both for the primary and the secondary components and tested them for the instability against radial and nonradial oscillations.

The best fit of the theoretical and observed frequency ranges is achieved for models with $T_{\text{eff}} \approx 7800$ K or slightly higher, in agreement with photometric calibrations. The instability spans two or three radial orders from p_4 to p_6 for radial modes. Post-MS models with or without overshooting are preferable for the primary, but MS models with overshooting are also possible.

For the less luminous secondary component the instability range is wider and spans 5 to 7 radial orders from p_2

to p_8 . Models of different effective temperature are unstable at observed frequencies 26.184 and 26.732 cd $^{-1}$ which lie around radial modes p_5 to p_6 .

The main uncertainties of the results are caused by our crude treatment of the convective flux. We neglected the Lagrangian variation of the convective flux during an oscillation cycle. This assumption is not fulfilled in the hydrogen convective zone, which may lead to an incorrect estimate of the small contribution of this zone to the driving. To prove the results quantitatively, it is necessary to use a reliable theory of non-local time-dependent convection. We note also the nonlocal results by Kupka & Montgomery (2002), who point out the necessity to use very different values of the mixing-length parameter in the hydrogen and helium convection zones, if we still use local mixing-length theory. According to nonlocal studies of A-star envelopes, it is necessary to use a small value of this parameter in the hydrogen zone and a significantly higher value in the deeper helium zone. We plan to perform corresponding tests for the θ^2 Tau models. However, even with the present calculations and results we probably can exclude modes involving the second radial overtone (mode p_3) and lower-order modes, as well as all hot models of the primary with $T_{\text{eff}} > 8000$ K. The reason is that all these models are stable in the observed frequency range of 10.8 to 14.6 cd $^{-1}$.

ACKNOWLEDGEMENTS

It is a pleasure to thank F. Beichbuchner for assistance with the observations. We are grateful to W. A. Dziembowski for stimulating discussions. This investigation has been supported by the Austrian Fonds zur Förderung der wissenschaftlichen Forschung under project number P14546-PHY (MB) and the Polish Committee for Scientific Research under Grant 5-P03D-012-20(AAP).

REFERENCES

Alexander D. R., Ferguson J. W., 1994, ApJ, 437, 879
 Breger, M., 1993, in Butler C. J., Elliott I., eds, Stellar Photometry - Current Techniques and Future Developments, Cambridge University Press, 106
 Breger M., 2000, in Breger M., Montgomery M. H., eds, Delta Scuti and Related Stars, ASP Conf. Ser. 210, 3
 Breger M., 2002, Communications in Asteroseismology (Vienna), 141, 3 (Paper II)
 Breger M., Bischof K. M., 2002, A&A, in press

Breger M., Pamyatnykh A. A., 1998, A&A, 332, 958

Breger M., Huang L., Jiang S.-y., Guo Z.-h., Antonello E., Mancagazza L., 1987, A&A, 175, 117

Breger M., Garrido R., Huang L., Jiang S.-y., Guo Z.-h., Frueh M., Paparo M., 1989, A&A, 214, 209 (Paper I)

Breger M., Stich J., Garrido R., et al., 1993, A&A 271, 482

Breger M., Handler G., Garrido R., et al., 1999, A&A, 349, 225

Breger M., Garrido R., Handler G., et al., 2002, MNRAS, 329, 531

de Bruijne J. H. J., Hoogerwerf R., de Zeeuw P. T., 2001, A&A, 367, 111

Duerbeck H. W., 1978, IBVS, 1412, 1

Dziembowski W. A., 1977, Acta Astron., 27, 95

Dziembowski W. A., Goode P. R., 1992, ApJ, 394, 670

Ebbighausen E. G., 1959, Pub. Dom. Astrophys. Obs., 11, 235

Garrido R., Rodriguez E., 1996, MNRAS, 281, 696

Handler, G., et al., 1996, A&A, 307, 529

Handler, G., et al., 2000, MNRAS, 318, 511

Horan S., 1977, IBVS, 1232, 1

Horan S., 1979, AJ, 84, 1770

Houdek G. A., 2000, in Breger M., Montgomery M. H., eds, Delta Scuti and Related Stars, ASP Conf. Ser. 210, 454

Iglesias C. A., Rogers F. J., 1996, ApJ, 464, 943

Kennelly E. J., Walker G. A. H., 1996, PASP, 108, 327

Kovacs G., Paparo M., 1989, MNRAS, 237, 201

Królikowska M., 1992, A&A, 260, 183

Kupka F., Montgomery M. H., 2002, MNRAS, 330, L6

Lastennet E., Valls-Gabaud D., Lejeune Th., Oblak E., 1999, A&A, 349, 485

Lebreton Y., Fernandes J., Lejeune T., 2001, A&A, 374, 540

Li Z.-p., Zhou A.-y., Yang D., 1997a, Acta Astrophys. Sinica, 17, 166

Li Z.-p., Zhou A.-y., Yang D., 1997b, PASP, 109, 217

Michel E., Hernández M. M., Houdek G., et al., 1999, A&A, 342, 153

Moon T. T., Dworetsky M. M., 1985, MNRAS, 217, 305

Pamyatnykh A. A., 2000, in Breger M., Montgomery M. H., eds, Delta Scuti and Related Stars, ASP Conf. Ser. 210, 215

Pérez Hernández F., Claret A., Hernández M. M., Michel E., 1999, A&A, 346, 586

Perryman M. A. C., et al., 1998, A&A, 331, 81

Peterson D. M., Stefanik R. P., Latham D. W., 1993, AJ, 105, 2260

Poretti E., Buzasi D., Laher R., Catanzarite J., Conrow T., 2002, A&A, 382, 157 (Paper III)

Rogers F. J., Swenson F. J., Iglesias C. A., 1996, ApJ, 456, 902

Soufi F., Goupil M.-J., Dziembowski W. A. 1998, A&A, 334, 911

Sperl M., 1998, Communications in Asteroseismology (Vienna), 111, 1

Stellingwerf R. F., 1984, ApJ, 277, 322

Torres G., Stefanik R. P., Latham D. W., 1997, ApJ, 485, 167